Protein Photocontrol

DOI: 10.1002/anie.201301490

Different Photochemical Events of a Genetically Encoded Phenyl Azide Define and Modulate GFP Fluorescence**

Samuel C. Reddington, Pierre J. Rizkallah, Peter D. Watson, Rachel Pearson, Eric M. Tippmann, and D. Dafydd Jones**

Genetically encoded photocontrol of protein function, known as optogenetics,[1] is a powerful approach for modulating biological processes with both high temporal and spatial resolution. Currently, optogenetics relies on a limited number of cofactor-dependent light sensitive proteins such as opsin channels[2] and LOV domains,[1b] which may restrict the general application of the approach. The introduction of new photochemistry intrinsic to the protein sequence through a reprogrammed genetic code[3] is an attractive alternative. A classic non-genetic approach involved the use of phenyl azides as photo-crosslinking agents introduced post-translationally and non-specifically in vitro. Phenyl azide chemistry can now be genetically encoded at precise and defined positions in a protein through the use of the tyrosine derivative *p*-azido-L-phenylalanine[4] (Figure 1a) and has been used to site-specifically modify proteins.[5] However, photochemical effects remain relatively unexplored both in terms of reaction pathways and use in controlling protein activity. Photolysis of phenyl azide releases N_2 forming a reactive singlet nitrene that follows several characterized pathways (see Supporting Information, Scheme S1), the distribution of which depends on the local environment, ring-substituents, and temperature. Possible routes include reduction to an amine, C–H bond insertion, or ring expansion.

Photo-controllable autofluorescent proteins are currently desirable as molecular highlighters for high-resolution cell imaging.[6] Considerable effort is devoted to engineering such proteins[6,7] but some limitations persist including robustness and photoconversion properties of the base protein scaffold. Ideally, photocontrol would be engineered into a highly stable, monomeric, fast-folding autofluorescent protein such as superfolder GFP (sfGFP)[8] with fast photoconversion kinetics and high magnitude changes on the application of relatively low energy. Here we show that incorporation of a single phenyl azide chemical unit at defined residues instils light-controllable fluorescence output over the normally photostable sfGFP. Three residues were targeted for AzF incorporation (Figure 1b): Y66 (sfGFP^{Y66AzF}) that forms part

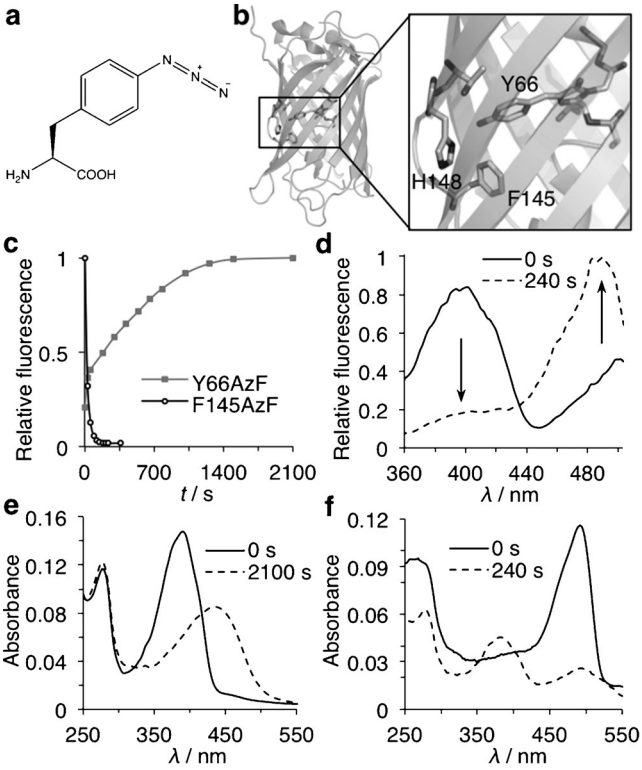

Figure 1. Protein engineering and spectroscopic properties of sfGFP^{AzF} variants. a) Structure of *p*-azido-L-phenylalanine (AzF). b) sfGFP residues targeted for AzF incorporation. c) Rate of photoactivation of sfGFP^{Y66AzF} (gray) and photodeactivation of sfGFP^{F145AzF} (black). Rates were calculated by plotting fluorescence emission (sfGFP^{Y66AzF} λ_{ex} 446 nm, λ_{em} 500 nm; sfGFP^{F145AzF} λ_{ex} 490 nm, λ_{em} 511 nm) against irradiation time. d) Excitation (λ_{em} 511 nm) spectra of sfGFP^{H148AzF} before and after irradiation. Absorption spectra of e) sfGFP^{Y66AzF} and f) sfGFP^{F145AzF} before (solid line) and after (dashed line) irradiation.

[*] S. C. Reddington, Dr. P. D. Watson, R. Pearson, Dr. D. D. Jones
School of Biosciences, Cardiff University, Cardiff (UK)
E-mail: jonesdd@cardiff.ac.uk
S. C. Reddington, Dr. E. M. Tippmann
School of Chemistry, Cardiff University, Cardiff (UK)
E-mail: tippmane@ipfw.edu
Dr. P. J. Rizkallah
School of Medicine, Cardiff University, Cardiff (UK)
Dr. E. M. Tippmann
Current address: Department of Chemistry, Indiana–Purdue University Fort Wayne, Fort Wayne, IN 46815 (USA)

[**] The authors would like to thank the BBSRC (BB/H003746/1 and BB/E007384), SARTRE (G0900868), and EPSRC (EP/J015318/1 and EP/H045848/1) for funding. S.C.R. was supported by a MRC studentship supplemented by School of Chemistry. The authors thank Prof. Barry Carpenter and Dr. Simon Pope for useful discussions concerning fluorescence modulation mechanisms, Dr. Ian Brewis and the CBS Proteomics Facility for mass spectrometry, DLS for access to the synchrotron facility, Dr. David Cole and Anna Fuller for assisting with crystallography, and Johanna Jones and Rebecca Thompson for help with preliminary experiments.

Supporting information for this article is available on the WWW under http://dx.doi.org/10.1002/anie.201301490.

WILEY ONLINE LIBRARY
© 2013 Wiley-VCH Verlag GmbH & Co. KGaA, Weinheim

of the chromophore; F145 (sfGFP^{F145AzF}) and H148 (sfGFP^{H148AzF}) that lie close in space to the chromophore (Figure 1b). The position of the phenyl azide in the protein determines both the effect on fluorescence and the reaction pathway sampled.

All variants were produced as soluble protein suggesting that sfGFP tolerated AzF at the chosen residue despite being buried in the protein interior. In the absence of AzF, no significant level of full-length sfGFP was produced due to premature termination of protein synthesis (Figure S1). On the application of low-intensity (6 W) broad spectrum UV light the sfGFP variants displayed one of three distinct light-dependent events: activation (sfGFP^{Y66AzF}), deactivation (sfGFP^{F145AzF}), and switching (sfGFP^{H148AzF}) (Figure 1c–f). sfGFP fluorescence was unchanged by irradiation in terms of intensity and spectral properties (Figure S2).

sfGFP^{Y66AzF} produced in the dark exhibited low fluorescence but on irradiation rapidly became highly fluorescent (Figure 1c), with a ca. 13-fold gain in brightness (Table S2). The spectral properties were different from sfGFP, with relatively broad, blue shifted excitation and emission peaks (Figure S3a,b). A major non-fluorescent absorbance peak at 390 nm was observed that converted to a 446 nm peak on irradiation (Figure 1e) with a λ_{em} of 498 nm, making it a close analogue of cyan FPs.[13] The extinction coefficient and quantum yield (QY) of photoactivated sfGFP^{Y66AzF} were significantly lower compared with sfGFP (Table S2) giving a brightness value of 3939 $M^{-1}cm^{-1}$. While not as bright as sfGFP, it still retains a useful fluorescence output after rapid photoactivation with low-intensity blue light within the context of the cell (see below). The crystal structures (see Table S3 for crystallographic statistics) of the dark and irradiated states of sfGFP^{Y66AzF} provided evidence of the photochemical event responsible for photoactivation. The structure of the dark state confirmed the presence of the azido group at its expected position in the chromophore (Figure 2a). The azido group may be responsible for the reduced fluorescence as the electron rich N^{α} is known to act as an excited-state quencher.[10] The in crystallo irradiated-state structure revealed that the benzyl ring of the chromophore was preserved and no cross-linked products were observed. No electron density was observed past N^{α} of the former azido group indicating the loss of N_2. The density at the *para* position of the ring was therefore modelled as $-NH_2$ (Figure 2b) so following the reduction route (Scheme S1). On loss of N_2 (Figure 2b), a water molecule appears to take the place of the azido group Nγ within H-bonding distance (3 Å) of the putative amine. This water is conserved in most GFP-like proteins that contain tyrosyl chromophores.[13] Reduction of phenyl azide to an phenylamine was substantiated by incorporation of the end-product equivalent *p*-amino-L-phenylalanine (AmF) at residue 66 in sfGFP; the fluorescence and absorbance spectra were very similar to the irradiated form of sfGFP^{Y66AzF} (Figure S4a,b) and to those observed for AmF incorporation at the same residue in original wild-type GFP.[11]

The sfGFP^{F145AzF} variant is produced fluorescent with spectral properties similar to sfGFP (Table S2) indicating addition of the azido group at the *para* position of the benzyl

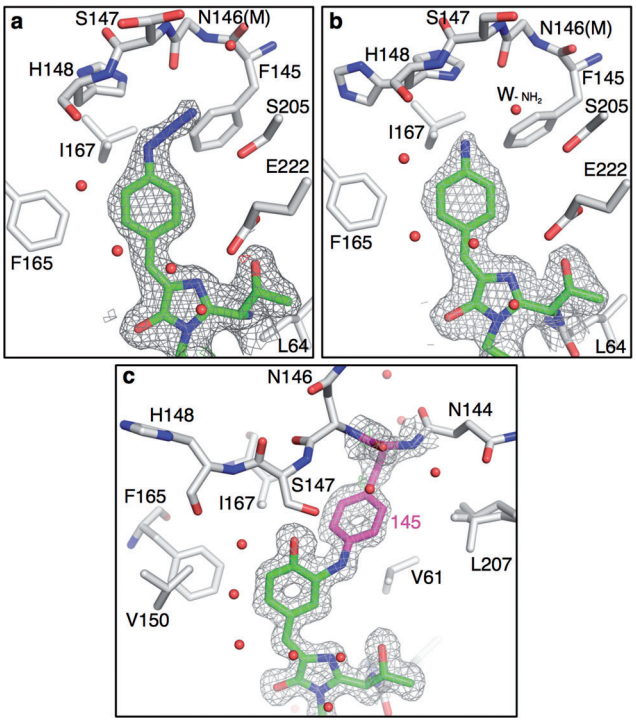

Figure 2. X-ray crystal structural study of photoconversion of sfGFP^{Y66AzF} and sfGFP^{F145AzF}. $2F_o-F_c$ maps of the a) dark (PDB 4J88) and b) irradiated (PDB 4J89) states of photoactivatable sfGFP^{Y66AzF} and c) irradiated state of photodeactivatable sfGFP^{F145AzF} (PDB 4J8A). Structures are colored by element with chromophore carbons colored green and residue 145 carbons in sfGFP^{F145AzF} colored pink. Neighboring residues are labeled and only the main chain of Asn146 is shown as indicated by (M). Multiple conformers of Ser147 and His148 were observed in the structures of a) dark-state and b) irradiated sfGFP^{Y66AzF}, respectively.

side chain of F145 had little effect on chromophore environment. On irradiation, sfGFP^{F145AzF} rapidly converts to a non-fluorescent form with at least a 53-fold loss in brightness (Figure 1c, Table S2). After irradiation, the 490 nm absorption peak decreases in intensity with the emergence of a non-fluorescent secondary peak at 386 nm (Figure 1f). The high-resolution (1.26 Å) crystal structure of in crystallo irradiated sfGFP^{F145AzF} suggests that the photochemical event causing deactivation differs from that observed for sfGFP^{Y66AzF}. The nitrene attacks the *meta* carbon of the chromophore phenol moiety to form an *N*-phenyl crosslink (Figure 2c). The reduction route is not taken given that incorporation of AmF at residue F145 results in spectral properties nearly identical to sfGFP (Figure S4c,d). Confirmation of crosslinking in irradiated sfGFP^{F145AzF} was indirectly confirmed by trypsin-digest MALDI-TOF. The fragment containing the chromophore could not be detected in any of the tested proteins, including sfGFP, which resulted in loss of the fragment housing residue 145 in the spectrum of irradiated sfGFP^{F145AzF} (Figure S5). The mechanism involves the phenolate form of the chromophore, as indicated by the λ_{max} at 490 nm for the dark form (Figure 1f).[13] The proximal electrophilic singlet nitrene attacks the delocalized, electron-rich chromophore resulting in C–H bond insertion at the

 © 2013 Wiley-VCH Verlag GmbH & Co. KGaA, Weinheim

phenolate *meta* position. Insertion of the out-of-plane phenyl nitrene (Figure 2c) (and associated nitrogen lone pair) gives the possibility of photoinduced proximate electron transfer as a non-radiative quenching pathway for the excited state. This is supported by the non-fluorescent absorbance peaks at 386/500 nm after irradiation (Figure 1f).

Programmed AzF incorporation in place of H148 (sfGFP^{H148AzF}) generated a variant displaying photoswitching with respect to excitation. Prior to irradiation, major and minor excitation peaks at 400 and 500 nm, respectively, were observed (Figure 1d). On irradiation, the 500 nm peak increased in intensity and blue-shifted by 10 nm while the 400 nm peak decreased by ca. 85% of its original intensity, with an isobestic point at 435 nm (Figure 1d). The λ_{em} remains at 511 nm, irrespective of excitation wavelength (400 nm or 500 nm) but intensity changes on irradiation in line with the changes in the two λ_{ex} resulting in a ca. 11-fold change in brightness (Table S2, Figure S6). Absorbance spectra before and after irradiation mirror changes in excitation spectra (Figure S6a). The likely mechanism of action is control over the protonation state of the chromophore in the ground state coupled with changes in chromophore environment in which H148 plays a role.[13] The photochemical endpoint of sfGFP^{H148AzF} that promotes the phenolate anion chromophore (λ_{ex} 485 nm) is unlikely to be the phenylamine. Incorporation of AmF at residue 148 to mimic the phenylamine generates distinct fluorescence and absorbance spectra compared to irradiated sfGFP^{H148AzF} (Figure S4e). This suggests that another currently unknown event is responsible for photoswitching in this variant.

The photoconversion characteristics of sfGFP^{Y66AzF} (activation) and sfGFP^{F145AzF} (deactivation) in vivo were demonstrated through live cell imaging of *E. coli*. Widefield fluorescence microscopy revealed that sfGFP^{Y66AzF} could be simultaneously activated and imaged with a 430 nm excitation filter (Figure 3a). Fluorescent activation was rapid with maximum intensity reached after 0.4 s. More precise control using laser scanning confocal microscopy (LSCM) allowed separate activation and visualization of sfGFP^{Y66AzF} at 405 nm (0.05 mW delivering 0.285 W cm^{-2} at the sample) and 488 nm (0.21 mW delivering 1.195 W cm^{-2}), respectively (Figure 3c). Fluorescent signal gain on photoactivation was ca. 20-fold with a $t_{1/2}$ of 5.0 s at 0.05 mW power (Figure 3c). Once activated, very little loss of fluorescence was observed during imaging (Figure 3c). Widefield fluorescence imaging of sfGFP^{F145AzF} revealed rapid deactivation whilst imaging using a 490 nm excitation filter with cells becoming essentially non-fluorescent after 0.5 s (Figure 3b). Using LSCM, sfGFP^{F145AzF} was imaged at 514 nm (0.02 mW delivering 0.114 W cm^{-2}) without deactivation, with deactivation initiated with a 405 nm laser at low energy output (0.63 mW delivering 3.584 W cm^{-2}). The $t_{1/2}$ for fluorescence deactivation was 9.0 s at 0.63 mW power input (Figure 3d). Fluorescence of individual cells producing either sfGFP^{Y66AzF} or sfGFP^{F145AzF} could be modulated on the application of a defined light source (Figure 3e,f,g). Increasing intensity of the photoconversion laser (405 nm; ≤1.61 mW delivering 9.159 W cm^{-2}), full photoactivation or -deactivation was achieved at high speed in a single step (400 Hz scan rate, 512 × 512 image; pixel dwell time of 5 μs). This paves the way for using these variants to examine high-speed cellular events through photoactivation and FRAP-like experiments using low-intensity blue light to modulate fluorescence, which is less damaging to the cell than UV normally used to photolyze phenyl azides.[14]

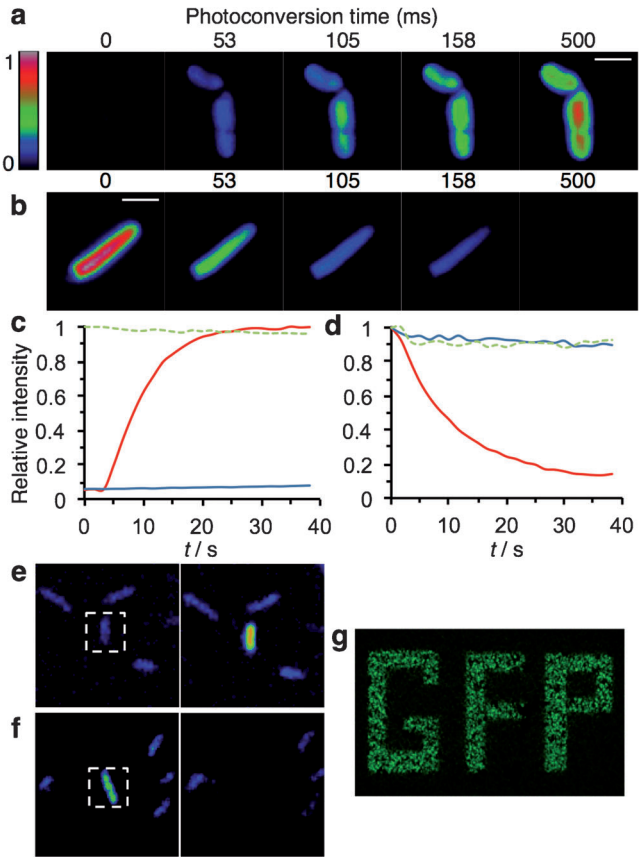

Figure 3. Photoconversion of sfGFP^{AzF} variants in live *E. coli* cells. Widefield fluorescence microscopy of cells producing a) photoactivating sfGFP^{Y66AzF} or b) photodeactivating sfGFP^{F145AzF}. Cells were photoconverted using a 430 nm and 488 nm filter, respectively, for the indicated amount of time. Images are false-colored (scale shown on the far left). Scale bars 2 μm. The rates of photoconversion were monitored by LSCM. Cells producing c) sfGFP^{Y66AzF} or d) sfGFP^{F145AzF} were photoconverted with a 405 nm laser (red trace). As a control, cells were not irradiated with 405 nm and only visualized before photoconversion (blue trace) at 488 nm (sfGFP^{Y66AzF}) or 514 nm (sfGFP^{F145AzF}). Cells producing sfGFP (green dashed) were irradiated at 405 nm under the same conditions as for photoconversion experiments. Photoconversion was quantified by monitoring individual cell fluorescence and plotting the value against time using Leica LCS software (sfGFP^{Y66AzF} $n = 65$, sfGFP^{F145AzF} $n = 100$). Spatial resolution of e) sfGFP^{Y66AzF} photoactivation and f) sfGFP^{F145AzF} photodeactivation. Regions of interest were selected for irradiation at 405 nm with the full field of view imaged with either a 488 nm (sfGFP^{Y66AzF}) or 514 nm (sfGFP^{F145AzF}) laser. g) "Writing" in a monolayer of cells producing sfGFP^{Y66AzF}.

The position and thus immediate environment within the buried sfGFP core sampled by genetically encoded phenyl azide profoundly influences the photochemical route taken resulting in distinct and useful effects on sfGFP fluorescence. Although the exact molecular determinants that favor

© 2013 Wiley-VCH Verlag GmbH & Co. KGaA, Weinheim

particular pathways is still being investigated, the observed influence of phenyl azide photolysis at engineered positions in a protein may open up new and general approaches for protein photocontrol, which our group is currently exploring. It therefore expands the use of genetically encoded azide chemistry in biological systems beyond Click chemistry-based bioconjugation and allies with the emerging discipline of optogenetics. The importance of autofluorescent proteins to cell imaging is clear, so our approach could be applied beyond sfGFP especially given the conserved nature of tyrosine in the chromophore. Reprogrammed genetic code systems can now be implemented in eukaryotic[5b] cells and whole animals[15] making both the sfGFP molecular highlighters developed herein and the general phenyl azide-based photocontrol of proteins of broad applicability.

Received: February 20, 2013
Published online: April 25, 2013

Keywords: expanded genetic code · green fluorescent protein · phenyl azide · photochemistry · protein engineering

[1] a) K. Deisseroth, *Nat. Methods* **2011**, *8*, 26 – 29; b) J. E. Toettcher, C. A. Voigt, O. D. Weiner, W. A. Lim, *Nat. Methods* **2011**, *8*, 35 – 38.
[2] P. Hegemann, A. Moglich, *Nat. Methods* **2011**, *8*, 39 – 42.
[3] a) L. Wang, A. Brock, B. Herberich, P. Schultz, *Science* **2001**, *292*, 498 – 500; b) L. Wang, J. Xie, P. G. Schultz, *Annu. Rev. Biophys. Biomol. Struct.* **2006**, *35*, 225 – 249; c) I. T. Yonemoto, E. M. Tippmann, *BioEssays* **2010**, *32*, 314 – 321.
[4] J. Chin, S. Santoro, A. Martin, D. King, L. Wang, P. Schultz, *J. Am. Chem. Soc.* **2002**, *124*, 9026 – 9027.
[5] a) M. D. Best, *Biochemistry* **2009**, *48*, 6571 – 6584; b) C. C. Liu, P. G. Schultz, *Annu. Rev. Biochem.* **2010**, *79*, 413 – 444; c) M. Boyce, C. R. Bertozzi, *Nat. Methods* **2011**, *8*, 638 – 642; d) S. C. Reddington, E. M. Tippmann, D. D. Jones, *Chem. Commun.* **2012**, *48*, 8419 – 8421.
[6] J. Lippincott-Schwartz, G. H. Patterson, *Trends Cell Biol.* **2009**, *19*, 555 – 565.
[7] a) G. H. Patterson, J. Lippincott-Schwartz, *Science* **2002**, *297*, 1873 – 1877; b) R. Ando, H. Hama, M. Yamamoto-Hino, H. Mizuno, A. Miyawaki, *Proc. Natl. Acad. Sci. USA* **2002**, *99*, 12651 – 12656.
[8] J. Pédelacq, S. Cabantous, T. Tran, T. Terwilliger, G. Waldo, *Nat. Biotechnol.* **2006**, *24*, 79 – 88.
[9] S. J. Miyake-Stoner, C. A. Refakis, J. T. Hammill, H. Lusic, J. L. Hazen, A. Deiters, R. A. Mehl, *Biochemistry* **2010**, *49*, 1667 – 1677.
[10] a) K. Sivakumar, F. Xie, B. M. Cash, S. Long, H. N. Barnhill, Q. Wang, *Org. Lett.* **2004**, *6*, 4603 – 4606; b) F. Xie, K. Sivakumar, Q. B. Zeng, M. A. Bruckman, B. Hodges, Q. Wang, *Tetrahedron* **2008**, *64*, 2906 – 2914.
[11] L. Wang, J. Xie, A. Deniz, P. Schultz, *J. Org. Chem.* **2003**, *68*, 174 – 176.
[12] a) J. Wang, G. Burdzinski, Z. D. Zhu, M. S. Platz, C. Carra, T. Bally, *J. Am. Chem. Soc.* **2007**, *129*, 8380 – 8388; b) V. Voskresenska, R. M. Wilson, M. Panov, A. N. Tarnovsky, J. A. Krause, S. Vyas, A. H. Winter, C. M. Hadad, *J. Am. Chem. Soc.* **2009**, *131*, 11535 – 11547.
[13] a) R. Y. Tsien, *Annu. Rev. Biochem.* **1998**, *67*, 509 – 544; b) J. H. Bae, M. Rubini, G. Jung, G. Wiegand, M. H. J. Seifert, M. K. Azim, J. S. Kim, A. Zumbusch, T. A. Holak, L. Moroder, R. Huber, N. Budisa, *J. Mol. Biol.* **2003**, *328*, 1071 – 1081.
[14] N. Gritsan, M. Platz, *Chem. Rev.* **2006**, *106*, 3844 – 3867.
[15] a) A. Bianco, F. M. Townsley, S. Greiss, K. Lang, J. W. Chin, *Nat. Chem. Biol.* **2012**, *8*, 748 – 750; b) S. Greiss, J. W. Chin, *J. Am. Chem. Soc.* **2011**, *133*, 14196 – 14199.

 © 2013 Wiley-VCH Verlag GmbH & Co. KGaA, Weinheim